GEOPHYSICS, VOL. 59, NO. 3 (MARCH 1994); P. 428–438, 6 FIGS., 2 TABLES.

The squirt-flow mechanism: Macroscopic description

Jack Dvorkin*, Richard Nolen-Hoeksema*, and Amos Nur*

ABSTRACT

We introduce a poroelasticity model that incorporates the two most important mechanisms of solid/fluid interaction in rocks: the Biot mechanism and the squirt-flow mechanism. This combined Biot/squirt (BISQ) model relates compressional velocity and attenuation to the elastic constants of the drained skeleton and of the solid phase, porosity, permeability, saturation, fluid viscosity and compressibility, and the characteristic squirt-flow length. Squirt-flow length is a fundamental rock property that does not depend on frequency, fluid viscosity, or compressibility and is determined experimentally. We find that the viscoelastic response of many sandstones is dominated by the squirt-flow component of the BISQ mechanism and that the viscoelastic properties of these rocks can be expressed through a single dimensionless parameter $\omega R^2/\kappa$, where ω is angular frequency, R is the characteristic squirt-flow length, and κ is hydraulic diffusivity. The Biot mechanism alone does not give an adequate explanation of the observed velocity dispersion and attenuation, and the viscoelastic behavior of many sandstones.

INTRODUCTION

This paper is a sequel to our previous work (Dvorkin and Nur, 1993) where we introduced a poroelasticity model that unifies the Biot and the squirt-flow mechanisms of solid/fluid interaction. There are several reasons that make this combined Biot/squirt (BISQ) approach to poroelastic modeling important both methodologically and practically.

First, the Biot and the squirt-flow solid/fluid interactions have been traditionally treated separately. Yet, they are intimately interconnected by the pore fluid. Therefore, a consistent poroelasticity theory has to consider both mechanisms simultaneously.

Second, the traditional description of the squirt-flow mechanism has been based on *microscopic* properties (e.g., an individual pore geometry). It is important to relate the poroelastic behavior of rocks to *macroscopic* measurable parameters (e.g., permeability, porosity, saturation, and pore-fluid compressibility, density, and viscosity).

Third, in many cases the Biot theory greatly underestimates velocity dispersion and attenuation. A realistic estimate of dispersion is necessary, for example, when using experimental laboratory ultrasonic velocity measurements to interpret sonic field data (velocity/frequency dispersion) and when monitoring pore-fluid viscosity changes (e.g., thermal enhanced oil recovery) from velocity logs (velocity/viscosity dispersion). Realistic attenuation values provide an important input to reflection coefficient calculations (e.g., Kjartansson, 1979).

We wish to emphasize here that it is not only the discrepancies between observed and Biot-predicted attenuation and velocity dispersion that imply the importance of the squirt-flow mechanism. There is an additional qualitative factor: the viscoelastic behavior of rocks with fluids. Experiments show that the high viscosity of oil in Berea sandstones acts to shift the relaxation towards lower frequencies (Winkler, 1985). The opposite effect is predicted by the Biot theory. Another example is the observed increase in compressional velocity with increasing pore-fluid viscosity (Nur and Simmons, 1969). Again, the Biot theory predicts the opposite trend.

We offer a theory that helps to resolve the above-mentioned problems by combining the squirt flow and the Biot mechanisms in a unified (BISQ) model. The model is based on a heuristic scheme of these two mechanisms occurring simultaneously in a rock when a planar compressional wave propagates through it. We assume that the solid skeleton of the rock deforms uniaxially with the only nonzero component of the deformation in the direction of wave propagation. The pore fluid, however, can move not only parallel but also lateral to this direction (Figure 1a). This lateral flow component is associated with the squirting of the fluid from the pores compressed by the wave.

Manuscript received by the Editor April 13, 1992; revised manuscript received May 26, 1993.
*Department of Geophysics, Stanford University, Stanford, CA 94305-2215.

For a lateral pressure gradient to develop, we assume that pore pressure on the sides of a small homogeneous representative volume of the rock does not change in time. This condition is strictly valid in apparently fully saturated rocks with only small amounts of high compressibility gas in the pores—a situation quite typical in natural reservoirs. The squirt-flow pattern becomes more complex in saturated rocks without residual gas: pore fluid is squeezed from thin cracks into surrounding large pores or adjacent cracks of different orientation (Mavko and Nur, 1975). Pressure on the sides of a representative volume does change in time. The amplitude of pressure variation in large pores is much smaller than that in thin cracks. Therefore, in this case the BISQ model will give realistic quantitative estimates to velocity dispersion and attenuation.

A natural choice of the representative volume for the case under consideration is a cylinder with its axis parallel to the direction of wave propagation. The radius of this cylinder is the characteristic squirt-flow length (Figure 1a). The physical meaning of the characteristic squirt-flow length is the average length that produces the squirt-flow effect identical to the cumulative effect of squirt flow in pores of various shapes and sizes. This parameter is intimately related to the pore space geometry of a given rock. We assume that it is a fundamental rock property that does not depend on frequency and fluid characteristics, and thus can be determined experimentally. This concept is similar to the permeability concept where permeability cannot be measured directly, but can be found by matching the Darcy formula's predictions with fluid flow rate and pressure gradient measurements.

The BISQ model does not require an individual pore geometry: pore fluid dynamics are linked to permeability and the characteristic squirt-flow length. Therefore, we model the squirt-flow mechanism by using its *macroscopic* rather than microscopic description.

In this paper, we analyze and simplify our earlier solution (Dvorkin and Nur, 1993) to show that for frequencies smaller than Biot's characteristic frequency the viscoelastic properties of rocks can be expressed through a single dimensionless parameter that is a combination of angular frequency, the characteristic squirt-flow length, and hydraulic diffusivity. We theoretically explore the relative importance of the Biot and the squirt-flow components of fluid flow on a high-porosity sandstone sample (the Biot dispersion and attenuation typically increase with increasing porosity). The example shows that the squirt-flow component dominates even in high-porosity rocks.

We explore the influence of permeability on attenuation and show that the BISQ model can explain experimentally observed relations between these two parameters.

Finally, we modify the formulas for velocity and attenuation for partially saturated rocks. To do so, we assume that the saturated part of the representative cylindrical volume is also a cylinder of a smaller radius (Figure 1b), which decreases with decreasing saturation. We find good agreement between experimental attenuation data and our theoretical predictions.

THE BISQ MODEL—VELOCITY AND ATTENUATION

BISQ and Biot formulas

The BISQ model gives the following expressions for the fast P-wave velocity V_P and attenuation coefficient a (Dvorkin and Nur, 1993):

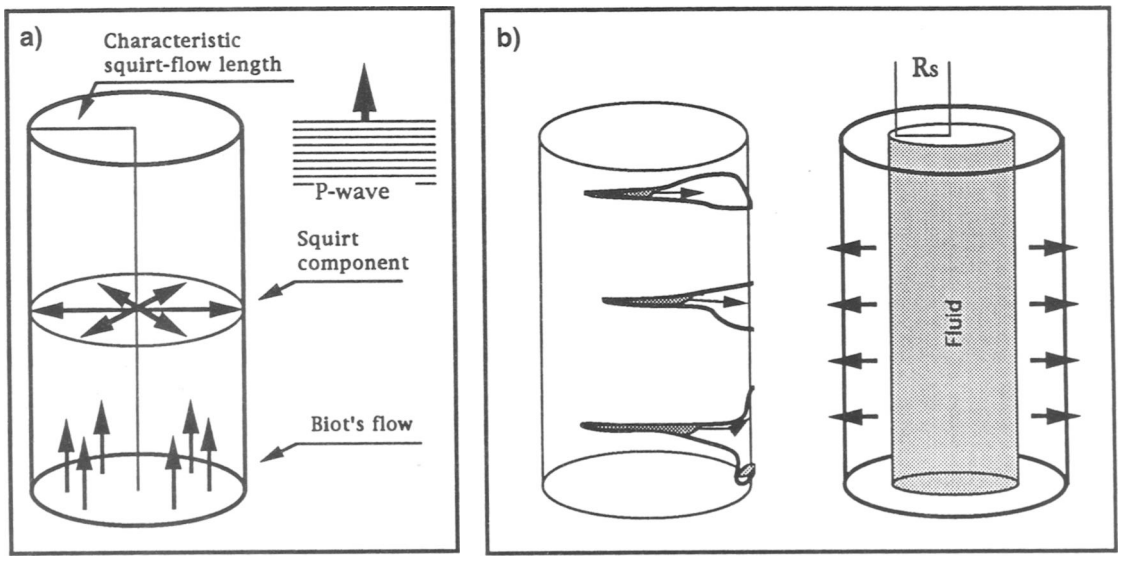

FIG. 1. The mechanical image of a representative cylinder used in the BISQ model: (a) Fluid flow in the cylinder—the Biot and the squirt components; a P-wave propagates parallel to the cylinder's axis. (b) Partial saturation—the radius of the fluid-filled cylinder decreases with decreasing saturation.

$$V_P = \frac{1}{Re(\sqrt{Y})}, \qquad a = \omega Im(\sqrt{Y}), \tag{1}$$

where

$$Y = -\frac{B}{2A} - \sqrt{\left(\frac{B}{2A}\right)^2 - \frac{C}{A}}, \qquad A = \frac{\phi F_{sq} M}{\rho_2^2},$$

$$B = \frac{F_{sq}\left(2\alpha - \phi - \phi\frac{\rho_1}{\rho_2}\right) - \left(M + F_{sq}\frac{\alpha^2}{\phi}\right)\left(1 + \frac{\rho_a}{\rho_2} + i\frac{\omega_c}{\omega}\right)}{\rho_2},$$

$$C = \frac{\rho_1}{\rho_2} + \left(1 + \frac{\rho_1}{\rho_2}\right)\left(\frac{\rho_a}{\rho_2} + i\frac{\omega_c}{\omega}\right), \tag{2}$$

$$F_{sq} = F\left[1 - \frac{2J_1(\lambda R)}{\lambda R J_0(\lambda R)}\right],$$

$$\lambda^2 = \frac{\rho_f \omega^2}{F}\left(\frac{\phi + \rho_a/\rho_f}{\phi} + i\frac{\omega_c}{\omega}\right).$$

In these equations, J_0 and J_1 are Bessel functions; ϕ is porosity; M is the uniaxial-strain modulus of the drained skeleton; R is the characteristic squirt-flow length;

$$\rho_1 = (1 - \phi)\rho_s, \qquad \rho_2 = \phi\rho_f;$$

ρ_s is the density of the solid (grain) material; ρ_f is the density of the fluid; ρ_a is the additional density introduced by Biot (1956) to quantify inertial coupling between the solid and the fluid; ω_c is Biot's characteristic angular frequency:

$$\omega_c = \frac{\mu\phi}{k\rho_f};$$

μ is the viscosity of the fluid; k is the permeability of the skeleton; ω is angular frequency; α is the poroelastic coefficient of effective stress:

$$\alpha = 1 - \frac{K}{K_s},$$

where K is the bulk modulus of the drained skeleton, and K_s is the bulk modulus of the solid phase;

$$F = \left(\frac{1}{\rho_f c_0^2} + \frac{1}{\phi Q}\right)^{-1}, \qquad \frac{1}{Q} = \frac{1}{K_s}\left(1 - \phi - \frac{K}{K_s}\right);$$

and c_0 is fluid acoustic velocity.

The inverse quality factor Q^{-1} is related to a and V_P as:

$$Q^{-1} = \frac{2aV_P}{\omega}.$$

These BISQ formulas give the Biot theory expressions for V_P and a when $F_{sq} = F$.

Low-frequency (squirt) formula

If frequency ω is much smaller than the Biot characteristic frequency ω_c:

$$\frac{\omega_c}{\omega} = \frac{\mu\phi}{k\rho_f\omega} \gg 1,$$

we can simplify equation (2) to obtain:

$$Y = \frac{\rho_s(1 - \phi) + \rho_f\phi}{M + F_{sq}\alpha^2/\phi}, \qquad F_{sq} = F\left[1 - \frac{2J_1(\xi)}{\xi J_0(\xi)}\right],$$

$$\xi = \sqrt{i}\sqrt{\frac{R^2\omega}{\kappa}}, \qquad \kappa = \frac{kF}{\mu\phi}. \tag{3}$$

In equation (3), κ can be identified as the diffusivity of the saturated rock (see Appendix A).

When reducing equation (2) to equation (3), we have eliminated the Biot component of the BISQ flow. The viscoelastic behavior of rock depends now on a single dimensionless parameter $\omega R^2/\kappa$ that only enters the expression for F_{sq}. Thus when substituting F instead of F_{sq} to obtain the Biot formulas from equation (3), we lose velocity-frequency dependence and find V_P being constant and equal to

$$\sqrt{\frac{M + F\alpha^2/\phi}{\rho_s(1 - \phi) + \rho_f\phi}},$$

which is the expression given by the Gassmann formula (White, 1983). Therefore, we can refer to equation (3) as the squirt-flow formula.

High-frequency formula

As we increase frequency, the imaginary part of λ in formula (2) becomes small and the Bessel function $J_0(\lambda R)$ in the denominator of the expression for F_{sq} approaches zero. As a result, we observe abrupt changes in V_P versus frequency in the high-frequency domain. This is the transverse resonance effect in the representative cylinder from the wave nature of the Biot formalism we used to relate the lateral (to the direction of a P-wave propagation) pressure gradient to pore-fluid displacement (Dvorkin and Nur, 1993). A similar resonance occurs in a pore when its (compressible) fluid component is compressed by a wave (Dvorkin et al., 1990).

We consider this resonance to be an artifact of our model because as yet there is no experimental evidence for it. This artifact can be eliminated by using

$$\lambda^2 = \frac{i\rho_f\omega\omega_c}{F} \tag{4}$$

instead of

$$\lambda^2 = \frac{\rho_f\omega^2}{F}\left(\frac{\phi + \rho_a/\rho_f}{\phi} + i\frac{\omega_c}{\omega}\right). \tag{5}$$

The physical meaning of this correction is employing Darcy's law instead of the Biot equation when relating lateral pressure gradient to pore-fluid displacement. This modification provides the needed smoothness to $V_P(\omega)$ curves. We feel it is physically justified as we are not concerned with the microscopic wave behavior of rock along the normal to the original P-wave. Our numerical experiments show that formula (4) can be used

instead of formula (5) to accurately calculate V_P and a in the whole frequency range.

BISQ, BIOT, AND SQUIRT—COMPARISON

Example

Experimental data.—We explore the dependence of V_P and Q^{-1} on frequency and fluid viscosity for a 36 percent porosity sandstone sample of 21 mdarcy permeability. Experimental ultrasonic (1 MHz) measurements were conducted on this water-saturated sample at 40 MPa confining pressure (Klimentos and McCann, 1990). The results are: V_P = 3121 m/s and the attenuation coefficient a = 4.54 dB/cm.

Theoretical calculations.—We used the elastic properties of the dry skeleton (bulk modulus K = 10.784 GPa, shear modulus G = 6.187 GPa) found by matching the computed and measured ultrasonic V_P values. The characteristic squirt-flow length R = 0.25 mm was determined by matching the computed and measured attenuation coefficients.

We calculated V_P and Q^{-1} versus frequency $f = \omega/(2\pi)$ for the sample saturated with water of viscosity 1 centipoise (cps), and two hypothetical fluids of viscosities 0.25 and 10 centipoise (Figure 2). We chose a high-porosity sample because the Biot attenuation and velocity/frequency dispersion are well-pronounced in such rocks. For smaller porosities (15–20 percent), the Biot attenuation and velocity/frequency dispersion are negligible compared to the experimental and BISQ-predicted values.

In Figure 2b, we plotted $Q^{-1}(f)$ and $V_P(f)$ computed from the BISQ formulas, and the Biot and squirt formulas for the water-saturated sample. The squirt Q^{-1} curve is shifted along the frequency axis relative to the BISQ curve. The BISQ-predicted and the squirt-predicted maximum Q^{-1} values are close to each other (and to the experimental measurements), whereas the Biot-predicted values are much smaller.

All three $V_P(f)$ curves in Figure 2 follow the same trend with a gradual transition from small, low-frequency to larger, high-frequency values. The BISQ and the squirt-predicted velocity-frequency dispersion values are close to each other. The Biot-predicted dispersion is much smaller.

The BISQ zero-frequency velocity limit is smaller than that predicted by Biot's theory and Gassmann's formula (Dvorkin and Nur, 1993). The reason is our assumption that there are small amounts of high-compressibility residual gas in rock.

As the viscosity of the pore fluid decreases (Figure 2a), the attenuation peak of the squirt curve shifts towards higher frequencies, whereas the Biot peak moves in the opposite direction. As a result, the BISQ Q^{-1} curve has two attenuation peaks: one resulting from the Biot and the other from the squirt Q^{-1} maxima. An analogous trend can be observed in $V_P(f)$ curves in Figure 2: the Biot low-to-high frequency transition region shifts towards lower frequencies as pore-fluid viscosity decreases, whereas the squirt curve exhibits the opposite behavior.

If pore-fluid viscosity is increased (Figure 2c), the squirt attenuation peak shifts towards lower frequencies and the Biot attenuation peak moves towards higher frequencies. The physical meaning of this disparity is that in rock with fluid, the Biot mechanism predicts solid/fluid coupling at low frequencies and decoupling at high frequencies, whereas the squirt-flow mechanism predicts the opposite behavior.

There is evidence that in some rocks the Biot-predicted viscoelastic behavior disagrees with observed trends. Winkler (1985) showed that in Berea sandstone relaxation shifts to lower frequencies as brine is substituted by high-viscosity oil. As we have shown above, the Biot theory predicts relaxation shifting to higher frequencies with increasing pore-fluid viscosity. Nur and Simmons (1969) showed that V_P in saturated Barre granite increases from 5080 to 5275 m/s as pore-fluid viscosity increases from 1 to 10^5 cps. Again, the Biot theory predicts velocity decrease with increasing pore-fluid viscosity.

This example shows that the BISQ model can better explain (both qualitatively and quantitatively) the observed viscoelastic behavior of rocks.

THE BISQ MODEL AND EXPERIMENTAL DATA

Velocity dispersion in sandstones

In this example, we use the data from 69 water-saturated jacketed sandstone samples tested at 1 MHz, 40 MPa confining pressure, and 1 MPa pore pressure (Han, 1986). The data also included porosity, clay content, density, and ultrasonic compressional and shear velocities in dry samples. The latter were used to compute the elastic properties of the dry skeletons.

Velocity versus frequency dispersion was calculated from the following limits:

1) the BISQ low-frequency velocity limit V_{01} (Dvorkin and Nur, 1993):

$$V_{01} = \sqrt{\frac{M}{(1-\phi)\rho_s + \phi\rho_f}};$$

2) the Biot (Gassmann) low-frequency velocity limit V_{02};
3) the BISQ high-frequency limit V_∞ (identical to Biot); and
4) the measured high-frequency velocity values in saturated samples $V_{\infty a}$.

We define:

1) apparent BISQ dispersion as $(V_{\infty a} - V_{01})/V_{\infty a}$,
2) predicted BISQ dispersion as $(V_\infty - V_{01})/V_{\infty a}$,
3) apparent Biot dispersion as $(V_{\infty a} - V_{02})/V_{\infty a}$,
4) predicted BISQ dispersion as $(V_\infty - V_{02})/V_{\infty a}$.

The predicted velocity dispersion is plotted against the apparent dispersion for the Biot and the BISQ models in Figure 3a and 3b, respectively. Straight lines in these plots correspond to the desired situation when the apparent values are identical to predicted values. It is clear from Figure 3 that the BISQ model gives much more accurate estimates of velocity/frequency dispersion than the Biot theory.

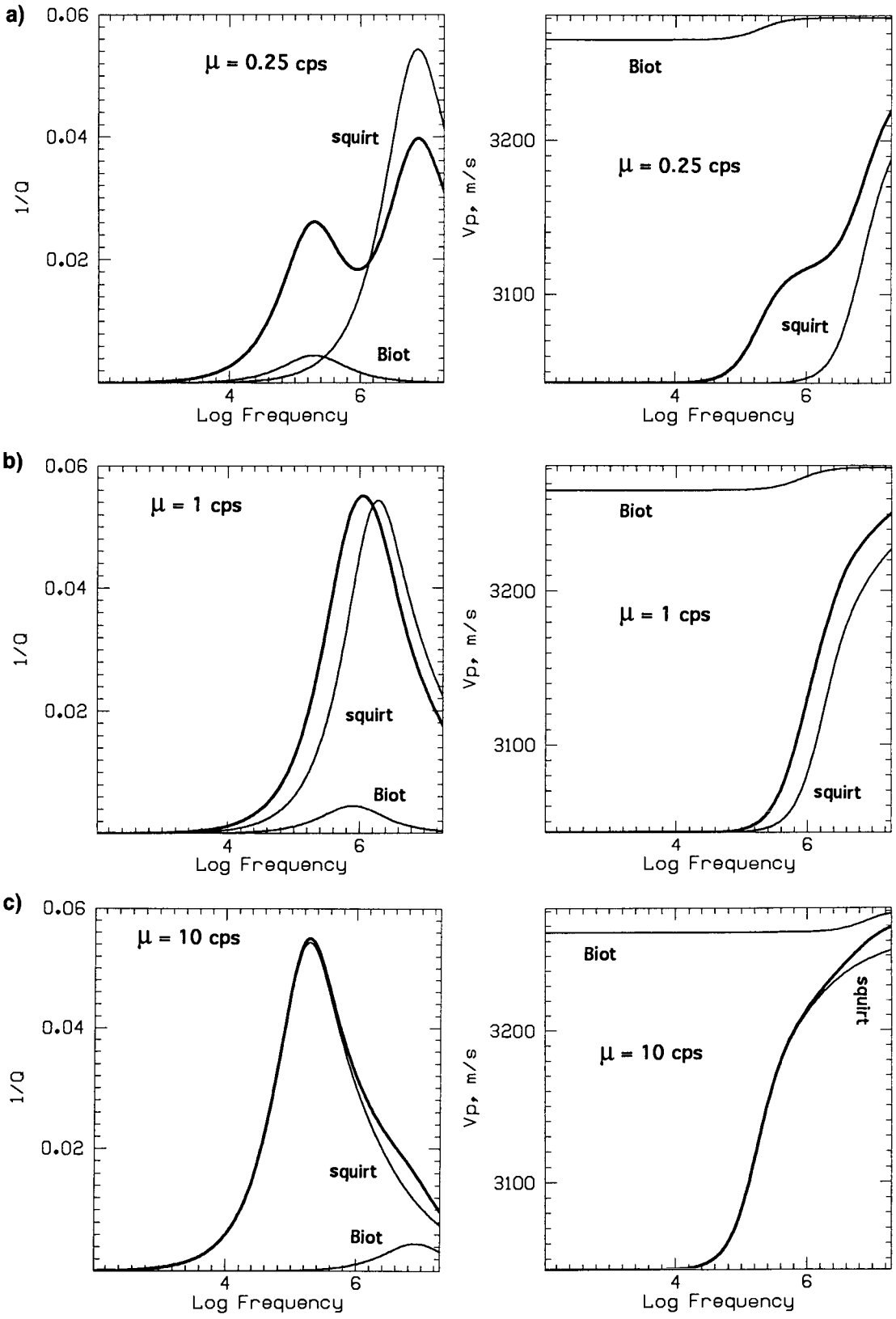

FIG. 2. Comparing the BISQ, the squirt, and the Biot formulas—Q^{-1} (left) and V_P (right) versus frequency in a high-porosity sandstone. Fluid viscosities are: (a) 0.25 cps, (b) 1 cps, and (c) 10 cps. Bold curves correspond to the BISQ model, thin marked curves correspond to the Biot and the squirt models.

Attenuation and permeability

Constant porosity sandstones.—In this example, we model the experimental results of Klimentos and McCann (1990) where ultrasonic (1 MHz) V_P and attenuation were measured as functions of permeability for 42 water-saturated sandstone samples at 40 MPa confining pressure. For selected 16 samples with porosities close to 15 percent, attenuation coefficient a systematically decreases with increasing permeability (Table 1). Yet, there is a scatter of a at low permeabilities.

Unfortunately, no data are available on the elastic properties of the skeletons that vary among the samples. We chose skeleton's bulk moduli by matching our theoretical predictions to experimental V_P data (Figure 4a). Poisson's ratio was fixed at 0.173—the value derived as an average from V_P and V_S data in nine dry sandstone samples of porosity about 15 percent (Han, 1986). The density and the bulk modulus of the grain material were fixed at 2650 kg/m^3 and 35 GPa, respectively. We varied the characteristic squirt-flow length among the samples by making it proportional to the average grain size given in Table 1 (proportionality coefficient 2.0 gave the best attenuation curve match).

Measured and calculated attenuation coefficients are plotted in Figure 4b (logarithmic permeability scale) and Figure 4c (linear permeability scale). The BISQ model gives realistic estimates of the actual attenuation data with the exception of the first two samples which have very low permeability. This discrepancy may be because of the difference between local (grain-scale) and global permeability. The difference may be especially great in these extremely low-permeability rocks (Berryman, 1988).

The following general trend can be observed in the data: a is small at small permeabilities, increasing to the maximum

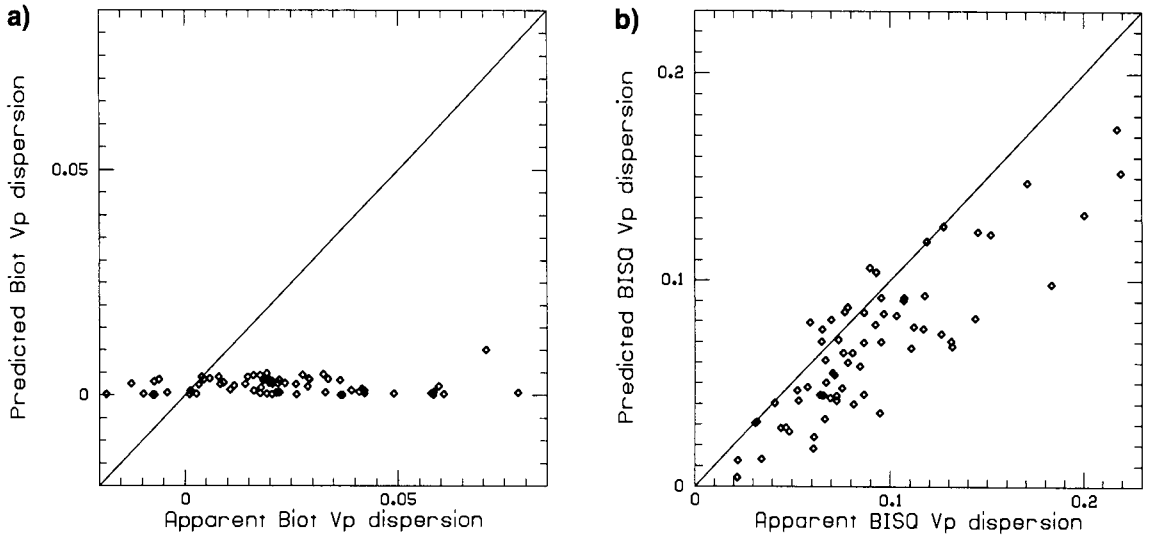

FIG. 3. Velocity/frequency dispersion in 69 sandstone samples (experimental data from Han, 1986). Predicted versus apparent dispersion (diamonds): (a) the Biot theory; (b) the BISQ model.

Table 1. The characteristics of 16 sandstone samples from Klimentos and McCann (1990). V_P measured at 1 MHz.

Sample no.	Porosity percent	Clay content percent	V_P m/s	Permeability mdarcy	Measured attenuation coefficient dB/cm	Average grain size mm
1	15.46	15.00	4152.	0.05	3.15	0.080
2	13.47	14.00	4498.	0.06	4.92	0.074
3	16.65	12.00	4010.	0.37	2.36	0.140
4	16.71	8.00	4381.	0.44	1.57	0.079
5	17.13	12.00	3933.	2.21	2.68	0.145
6	13.11	7.00	4666.	3.67	2.10	0.226
7	15.13	4.00	4794.	11.06	1.65	0.271
8	16.50	15.00	4149.	41.54	3.63	0.377
9	16.11	15.00	4152.	50.71	3.30	0.312
10	15.41	15.00	4246.	52.42	3.38	0.330
11	15.72	5.00	4564.	87.55	0.47	0.226
12	13.72	0.50	4950.	87.65	0.09	0.235
13	14.15	1.00	4960.	150.70	0.70	0.229
14	15.18	0.70	4942.	160.40	0.14	0.260
15	14.47	0.20	4788.	220.90	0.08	0.242
16	14.37	1.00	5078.	255.90	0.29	0.272

at intermediate permeabilities, and decreasing sharply for large permeabilities. The two sharp attenuation maxima at low permeabilities (Figure 4b) can be attributed to the variation of the elastic properties of the samples as seen in abrupt changes to V_P (Figure 4a).

This trend can be clearly seen in Figure 4d (the upper curve) where coefficient a is plotted against permeability for a hypothetical group of samples with changing permeability but fixed elastic properties. As permeability increases, the attenuation rises to its intermediate maximum and sharply drops afterwards to low values. This effect is similar to the squirt-flow attenuation/frequency function (Akbar et al., 1993): at low permeability, the pore fluid is unrelaxed and attenuation is small (corresponds to high frequencies); at high permeability, pore fluid is relaxed, which again results in small attenuation (corresponds to low frequencies); therefore, the attenuation maximum is located between these two limits (intermediate frequencies). We believe that this non-

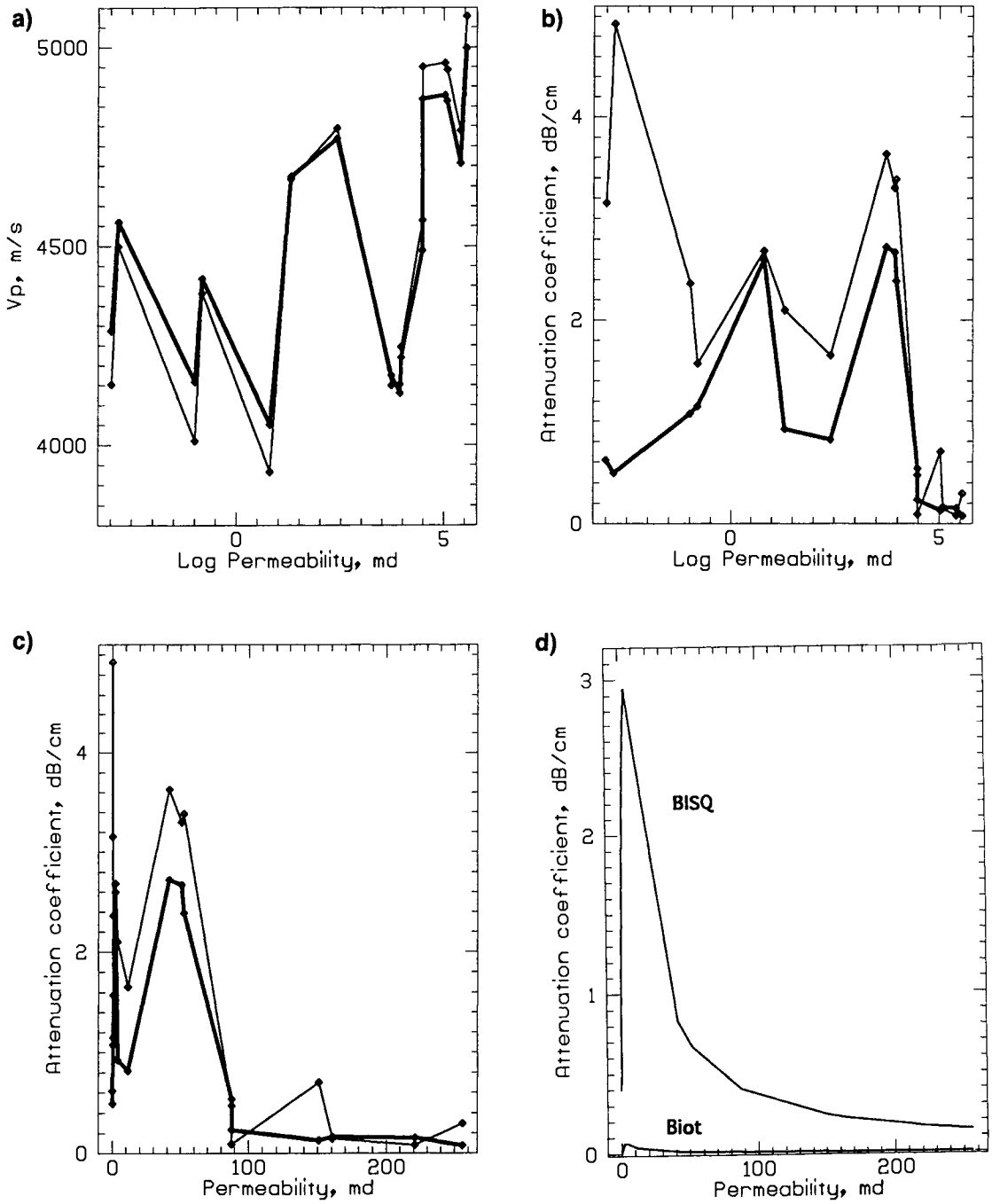

FIG. 4. Velocity/permeability and attenuation/permeability predictions in sandstone samples based on Klimentos and McCann (1990); bold lines—the BISQ-predicted values; thin lines—experimental data: (a) Compressional velocity versus permeability. (b) Attenuation coefficient versus permeability—log scale. (c) Attenuation coefficient versus permeability—regular scale. (d) Attenuation coefficient versus permeability—hypothetical samples.

monotonous attenuation/permeability dependence is one reason for the highly scattered experimental values of the attenuation coefficients at very low permeabilities.

It is important to state here that the Biot theory (Figure 4d, lower curve) gives attenuation values that are much smaller than those predicted by BISQ (Figure 4d, upper curve).

Fontainebleau sandstone.—In this example, we use experimental ultrasonic (0.5 MHz) measurements on five water-saturated Fontainebleau sandstone samples of varying porosity and permeability (Lucet, 1989). Confining pressure was 10 MPa. The experimental data are summarized in Table 2. The elastic properties of the samples were chosen to match the measured velocity values (Figure 5a).

The characteristic squirt-flow length 2.8 mm was chosen to match the maximum theoretical and experimental values of Q^{-1}. We kept this parameter constant among the samples. Again, the measured and the BISQ-predicted attenuation/permeability functions are close (Figure 5b).

The characteristic squirt-flow length appears to be very large in this case. This may be because Fontainebleau sandstone is a well-sorted rock with large grain size and regular pore space (Bourbie et al., 1987). It is this regularity that makes the heterogeneities large and thus causes the squirt-flow path to be as long as ten grain sizes.

The above two examples prove that there is a distinct connection between attenuation and permeability: generally, attenuation is small both at very small and very high permeabilities, and has a maximum at intermediate permeabilities.

INTRODUCING SATURATION

Theoretical formulas

One way of introducing partial saturation in the squirt-flow formalism is to assume that the characteristic squirt-flow length decreases from its initial value R in a fully saturated rock ($S = 1$) to $R_s < R$ at saturation $S < 1$. Using the mechanical image of a representative cylindrical volume of a rock (Figure 1a), we assume that the saturated part of this volume is also a cylinder of a smaller radius R_s (Figure 1b). We will assume in addition that this radius R_s is the characteristic squirt-flow length. Therefore, the characteristic squirt-flow length at saturation S is related to that in the fully saturated rock by

Table 2. The characteristics of five Fontainebleau sandstone samples from Lucet (1989). V_P, V_S, and compressional-wave attenaution quality factor measrued at 0.5 MHz.

Sample no.	Porosity percent	V_P m/s	V_S m/s	Permeability mdarcy	Compressional attenuation quality factor	Average grain size mm
1	6.7	5273.	3301.	6.	200.	0.25
2	13.6	4667.	2923.	670.	60.	0.25
3	14.8	4389.	2715.	720.	53.	0.25
4	15.5	4565.	2762.	1080.	83	0.25
5	22.0	4245.	2674.	2800.	240.	0.25

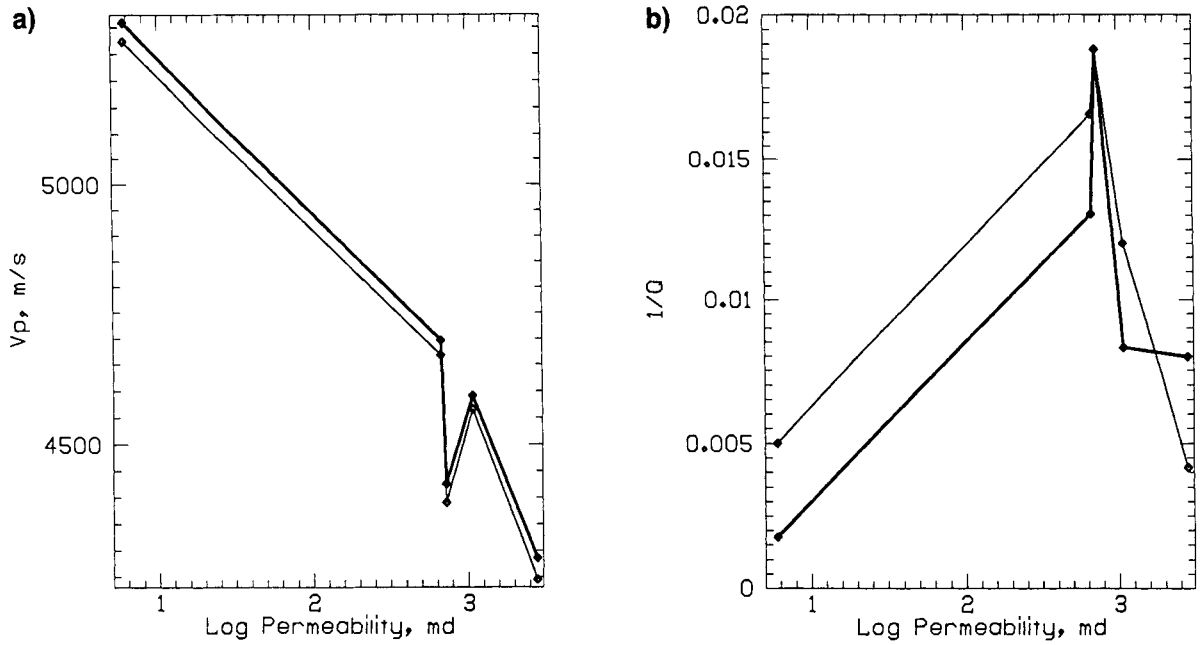

FIG. 5. Velocity/permeability and attenuation/permeability predictions in five water-saturated Fontainebleau sandstone samples of varying porosity and permeability (experiments of Lucet, 1989); bold lines—the BISQ-predicted values, thin lines—experimental data: (a) Matched velocities. (b) Measured and computed Q^{-1}.

$$R_s = R\sqrt{S}. \tag{6}$$

The squirt-flow formula (3) can be modified to include partial saturation by:

1) using the effective density of the fluid/gas mixture $S\rho_f$ instead of fluid density ρ_f and
2) using pore-pressure averaged with respect to r in the domain $0 < r < R$ instead of that averaged in the domain $0 < r < R_s$, and thus using $SF_{sq}\alpha^2/\phi$ instead of $F_{sq}\alpha^2/\phi$.

After these modifications, we find at saturation S:

$$V_P = \frac{1}{Re(\sqrt{Y})}, \qquad a = \omega Im(\sqrt{Y}), \tag{7}$$

where

$$Y = \frac{\rho_s(1-\phi) + S\rho_f\phi}{M + SF_{sq}\alpha^2/\phi}, \qquad F_{sq} = F\left[1 - \frac{2J_1(\xi)}{\xi J_0(\xi)}\right],$$

$$\xi = \sqrt{i}\sqrt{\frac{SR^2\omega}{\kappa}}, \qquad \kappa = \frac{kF}{\mu\phi}.$$

Experimental data

We explore the effect of saturation on velocity and attenuation in a Fort Union sandstone sample using the experimental data of Murphy (1984). Extensional (V_e) and shear (V_S) velocities and inverse quality factors (Q_e^{-1} and Q_s^{-1}, respectively) have been measured using a resonant bar technique at 5 kHz and water saturation between 0 and 100 percent.

Fort Union sandstone is a poorly sorted fluvial subgraywacke with porosity 8.5 percent and mean grain size between 0.125 and 0.15 mm. The density and the bulk modulus of the grain material are 2650 kg/m^3 and 35 GPa, respectively. The elastic properties of the skeleton calculated by matching V_e and V_S at 10 percent saturation (Figure 6a) are: bulk modulus 7.93 GPa and shear modulus 11.0 GPa. We used the "wet" data here because the elastic constants of a dry skeleton change with the addition of small amounts of moisture (Murphy, 1982).

There is no explicit data on the permeability of the Fort Union sandstone sample. We assume that the permeability is in the range of 0.01–0.1 mdarcy, as in the Spirit River sandstone samples, which are lithologically similar to Fort Union sandstone (Murphy, 1982). Two of the samples have porosity 0.071 and 0.054, and permeability 0.058 and 0.021 mdarcy, respectively. Therefore, we have chosen the permeability of the Fort Union sandstone as 0.04 mdarcy.

We obtained theoretical V_e and Q_e^{-1} from the BISQ-predicted V_P and Q^{-1} and experimentally measured V_S and Q_s^{-1}. Q_e^{-1} was calculated from

$$\frac{(1-\nu_s)(1-2\nu_s)}{Q} = \frac{1+\nu_s}{Q_e} - \frac{2\nu_s(2-\nu_s)}{Q_s},$$

where ν_s is Poisson's ratio at varying saturation (Winkler and Nur, 1979).

The characteristic squirt-flow length 0.5 mm gave the best correlation between the measured and the BISQ-predicted inverse quality factor values (Figure 6b).

The shape of the modeled $V_e(S)$ curve repeats the shape of the relation obtained experimentally (Figure 6a). However the values of computed V_e are larger than those from

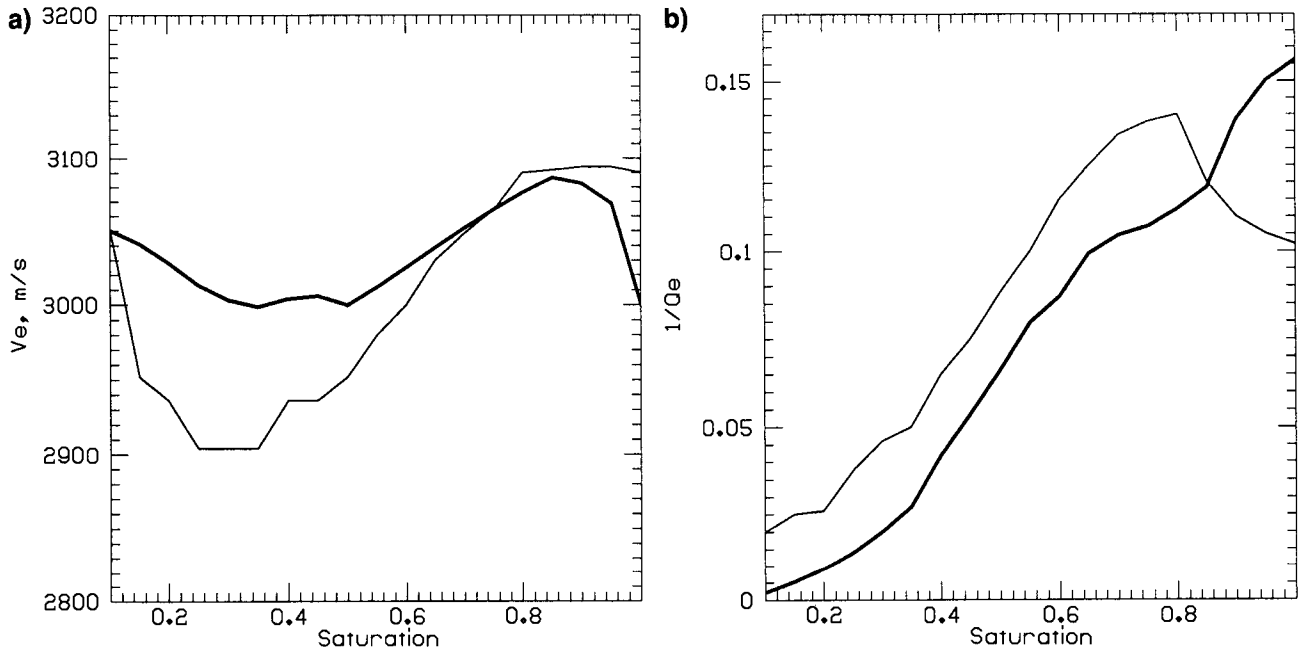

FIG. 6. The effect of saturation on velocity and attenuation in a Fort Union sandstone sample (experiments of Murphy, 1984). Bold lines—the BISQ predictions; thin lines—experiment. (a) Velocity. (b) Inverse quality factor.

experimental data at intermediate saturations. Still, our model gives much better correlation with the experiment than the Biot-Gassmann-Domenico prediction (Murphy, 1984). The computed values of Q_e^{-1} closely follow the trend and the magnitude of the experimental data at saturations below 0.8 (Figure 6b). Figure 6 shows discrepancies between the BISQ-predicted and the experimental values at high saturations ($S > 0.8$). These may be due to the fact that at saturations close to 1.0, resonant bar measurements cannot be directly interpreted in terms of waves propagating in an infinite medium. The reason is the "open pore condition" at the surface of a bar (White, 1986).

CONCLUSIONS

The two main features of the BISQ model are:

1) pore fluid simultaneously participates in the Biot-type flow and in the squirt-type flow; and
2) the model requires fewer inputs than previous squirt-flow models—it is independent of assumptions about idealized pore geometries and aspect ratios, and relates attenuation and velocity dispersion to macroscopic measurable rock properties.

The key assumption of the model is that the characteristic squirt-flow length R is a fundamental rock property that does not depend on frequency, fluid viscosity, or compressibility. Therefore, this newly introduced parameter can be found by matching the experimental measurements of velocity and/or attenuation (at a given frequency) with their theoretical values. We feel that this assumption is justified by (1) generally good correlation between the model and data (we have shown that R can be determined at one experimental point and used afterwards to theoretically predict the poroelastic behavior of the rock), and (2) the fact that the formulation is entirely in terms of measurable bulk properties only, without the need for poorly determined parameters such as fracture geometry.

It is important to emphasize that in a given rock, R generally depends on effective pressure. Its value will be affected by pressure crack lengths and grain contact configurations.

The additional assumptions are:

1) the mineral matrix is elastically homogeneous and isotropic;
2) permeability is the same in all directions; and
3) the compressibility of gas in partially (or apparently fully) saturated pores is high as compared to pore fluid compressibility.

The main results are:

1) the model realistically predicts high attenuation and velocity dispersion observed in many experiments;
2) the model describes the poroelastic behavior of rocks through a single combination of frequency, diffusivity, and the characteristic squirt-flow length;
3) the squirt-flow mechanism dominates the Biot mechanism and is responsible for measuring large velocity dispersion and attenuation values;
4) the model explains a number of experimentally observed trends such as increasing compressional velocity and shift in relaxation to lower frequencies with increasing pore-fluid viscosity; and
5) there is a distinct relation between attenuation and permeability: attenuation is small at small permeabilities, increases to a maximum at intermediate permeabilities, and decreases sharply for large permeabilities.

The BISQ model is an improved attempt to quantitatively and consistently relate the features of the squirt-flow mechanism to macroscopically measurable rock and fluid properties, and frequency. Additional research effort is needed to accurately model squirt flow in saturated rocks without residual gas, and to rigorously relate global permeability and diffusivity to permeability and diffusivity that control the Biot/squirt-fluid dynamics.

We believe that an important potential of the BISQ model is in contributing to the rock physics niche of geophysical remote sensing methods. We have shown that at a given frequency, both velocity and attenuation may change strongly with the changing pore fluid viscosity. Therefore, by employing the BISQ formulas, we can, in principle, use these seismic signatures to monitor changes in fluid viscosity (and thus temperature). Such monitoring will be appropriate, for example, in a heavy oil reservoir subject to thermal enhanced oil recovery treatment (Nur, 1989; Dvorkin and Nur, 1993).

ACKNOWLEDGMENTS

We thank Gary Mavko, Nabil Akbar, and Jim Berryman for helpful discussions, and the reviewers for their useful comments. Our special thanks to Ken Mahrer for careful and constructive reviews. This work was sponsored by the Gas Research Institute Contract No. 5087-260-1635.

REFERENCES

Akbar, N., Dvorkin, J., and Nur, A., 1993, Relating P-wave attenuation to permeability: Geophysics, **58**, 20–29.
Berryman, J. B., 1988, Seismic wave attenuation in fluid-saturated porous media: PAGEOPH, **128**, 423–423.
Biot, M. A., 1956, Theory of propagation of elastic waves in a fluid-saturated porous solid. a. Low-frequency range, b. Higher frequency range: J. Acoust. Soc. Am., **28**, 168–191.
Bourbie, T., Coussy, O., and Zinzner, B., 1987, Acoustics of porous media: Gulf Publ. Co.
Dvorkin, J., Mavko, G., and Nur, A., 1990, The oscillations of a viscous compressible fluid in an arbitrarily-shaped pore: Mech. of Materials, **9**, 165–179.
Dvorkin, J., and Nur, A., 1993, Dynamic poroelasticity: A unified model with the squirt and the Biot mechanisms: Geophysics, **58**, 524–533.
Han, D., 1986, Effects of porosity and clay content on acoustic properties of sandstones and unconsolidated sediments: Ph.D. thesis, Stanford University.
Klimentos, T., and McCann, C., 1990, Relationships among compressional wave attenuation, porosity, clay content, and permeability in sandstones: Geophysics, **55**, 998–1014.
Kjartansson, E., 1979, Attenuation of seismic waves in rocks and applications in energy exploration: Ph.D. thesis, Stanford University.
Lucet, N., 1989, Vitesse et attènuation des ondes èlastiques soniques et ultrasoniques dans les roches sous pression de confinement: Thesé de Doctorat de l'Universitè Paris 6.
Mavko, G., and Nur, A., 1975, Melt squirt in asthenosphere: J. Geophys. Res., **80**, 1444–1448.
Murphy, W. F., III, 1982, Effects of microstructure and pore fluids on the acoustic properties of granular sedimentary material: Ph.D. thesis, Stanford University.

——— 1984, Acoustic measures of partial gas saturation in tight sandstones: J. Geophys. Res., **89**, 11549–11559.
Nur, A., 1989, Four-dimensional seismology and (true) direct detection of hydrocarbons, The petrophysical basis: The Leading Edge, **8**, no. 30–36.
Nur, A., and Simmons, G., 1969, The effect of viscosity of a fluid phase on velocity in low porosity rocks: Earth Plan. Sci. Lett., **7**, 99–108.
White, J. E., 1983, Underground sound: Elsevier Science Publ. Co.
——— 1986, Biot-Gardner theory of extensional waves in porous rods: Geophysics, **51**, 742–745.
Winkler, K. W., 1985, Dispersion analysis of velocity and attenuation in Berea sandstone: J. Geophys. Res., **90**, 6793–6800.
Winkler, K. W., and Nur, A., 1979, Pore fluids and seismic attenuation in rocks: Geophys. Res. Lett., **6**, 1–4.

APPENDIX

DIFFUSIVITY OF ROCK

The 1-D equation of a fluid's mass conservation in a saturated porous medium is:

$$\frac{\partial(\rho_f\phi)}{\partial t}+\frac{\partial(\rho_f q)}{\partial x}=0,$$

where t is time; x is a spatial coordinate; and q is the volumetric filtration rate in the x-direction. The flow rate q is related to pore pressure gradient by Darcy's law:

$$q=-\frac{k}{\mu}\frac{\partial P}{\partial x}.$$

These two relations lead to the following diffusion equation:

$$\frac{\partial P}{\partial t}=\frac{k}{\phi\mu(\beta_f+\beta_m)}\frac{\partial^2 P}{\partial x^2},$$

where

$$\beta_f=\frac{1}{\rho_f}\frac{\partial\rho_f}{\partial P}=\frac{1}{\rho_f c_0^2}$$

is fluid compressibility and

$$\beta_m=\frac{1}{\phi}\frac{\partial\phi}{\partial P}$$

is pore-volume compressibility. The combination

$$\frac{\kappa}{\phi\mu(\beta_f+\beta_m)}$$

is called the diffusivity κ of the saturated porous medium.

The pore-volume compressibility can be expressed through the poroelastic constant Q as

$$\beta_m=\frac{1}{\phi Q},$$

which follows from the relation among porosity differential $d\phi$, deformation differential de, and pore pressure differential dP (Dvorkin and Nur, 1993):

$$d\phi=\alpha\, de+dP/Q.$$

Therefore,

$$F^{-1}=\frac{1}{\rho_f c_0^2}+\frac{1}{\phi Q}=\beta_f+\beta_m$$

and

$$\kappa=\frac{kF}{\mu\phi}.$$